

VIDEOZOOMER: REINFORCEMENT-LEARNED TEMPORAL FOCUSING FOR LONG VIDEO REASONING

000
001
002
003
004
005 **Anonymous authors**
006 Paper under double-blind review
007
008
009
010
011

ABSTRACT

012 Multimodal Large Language Models (MLLMs) have achieved remarkable
013 progress in vision-language tasks yet remain limited in long video understand-
014 ing due to the limited context window. Consequently, prevailing approaches tend
015 to rely on uniform frame sampling or static pre-selection, which might overlook
016 critical evidence and unable to correct its initial selection error during its reasoning
017 process. To overcome these limitations, we propose VideoZoomer, a novel agentic
018 framework that enables MLLMs to dynamically control their visual focus during
019 reasoning. Starting from a coarse low-frame-rate overview, VideoZoomer invokes
020 a temporal zoom tool to obtain high-frame-rate clips at autonomously chosen mo-
021 ments, thereby progressively gathering fine-grained evidence in a multi-turn inter-
022 active manner. Accordingly, we adopt a two-stage training strategy: a cold-start
023 supervised fine-tuning phase on a curated dataset of distilled exemplar and reflec-
024 tion trajectories, followed by reinforcement learning to further refine the agentic
025 policy. Extensive experiments demonstrate that our 7B model delivers diverse
026 and complex reasoning patterns, yielding strong performance across a broad set
027 of long video understanding and reasoning benchmarks. These emergent capabili-
028 ties allow it to consistently surpass existing open-source models and even rival
029 proprietary systems on challenging tasks, while achieving superior efficiency un-
030 der reduced frame budgets.
031
032

1 INTRODUCTION

033 With a clear task in mind, humans can efficiently navigate long and complex visual streams by
034 dynamically allocating attention, selectively identifying salient events such as decisive actions in a
035 sports match or key explanations in a lengthy lecture, while filtering out redundancy. This goal-
036 directed ability underlies effective and efficient visual reasoning, as widely documented in cognitive
037 science (Kietzmann et al., 2018), remains difficult to achieve in artificial intelligence. Although
038 MLLMs perform strongly on image (Bai et al., 2025; Chen et al., 2024) and short-video tasks (Zhang
039 et al., 2023), they remain constrained in long-video comprehension tasks mainly due to their limited
040 context window (OpenAI, 2024; Reid et al., 2024).
041

042 The most common strategy to address this challenge is uniform frame sampling (Zhang et al.,
043 2024b;c), which selects frames at fixed intervals (e.g., two frames per second) to construct a sub-
044 set that fits within context window. Nevertheless, this strategy is inherently limited, as it assumes
045 all moments are equally important and further risks overlooking short but critical events while al-
046 locating context budget to redundant clip segments. To address these limitations, prior work has
047 investigated adaptive frame selection (Yu et al., 2024; Hu et al., 2025a; Tang et al., 2025), where a
048 lightweight selector module, conditioned on the text query, identifies salient frames before reason-
049 ing. While improving over uniform sampling, these methods are still inefficient because they are
050 designed to select a fixed number of frames regardless of the problem’s complexity. Second, the
051 design remains static and non-interactive. If the initial choice is suboptimal or misses key details,
052 the model has no mechanism to correct the error or revisit the video. This fundamentally limits its
053 performance on complex tasks that require iterative evidence gathering.

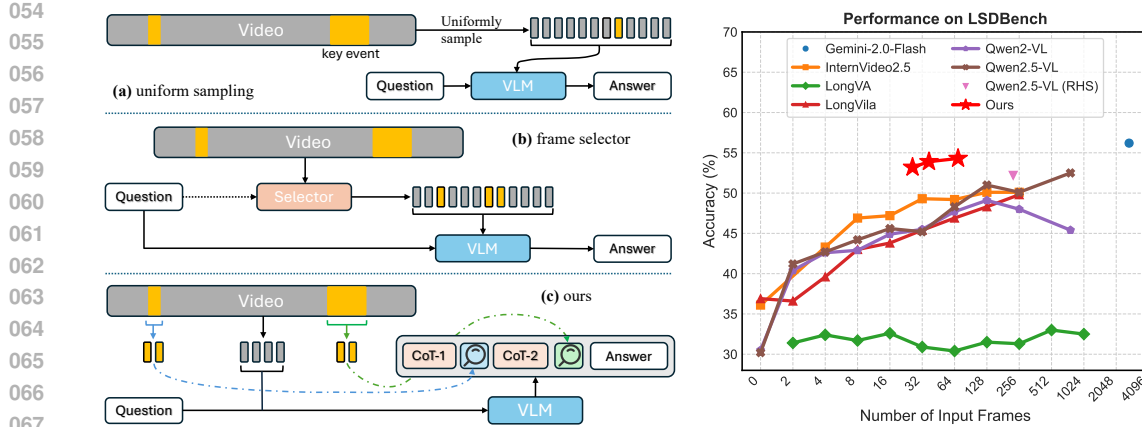


Figure 1: **Left:** Conceptual comparison of three long video reasoning frameworks: (a) uniform sampling, (b) with frame selector, and (c) VideoZoomer (Ours). **Right:** Performance comparison of VideoZoomer against various baseline models under different frame budgets on LSDBench.

To overcome the rigidity and inefficiency of prior methods, we propose VideoZoomer, a novel framework that empowers an MLLM to autonomously and dynamically control its visual focus during its reasoning process. As illustrated in Figure 1 (Left), instead of being a passive recipient of pre-selected frames, our model acts as an active agent. This yields two primary advantages: (i) It is highly efficient: the agent begins with a coarse overview of low frame rates, only consuming a significant context budget when it decides to invoke a `<video_zoom>` tool. This on-demand approach ensures that the model’s context window is used dynamically and judiciously. (ii) It is more performant: by learning a policy to request high-frame-rate clips of specific moments, the agent can correct initial oversights and gather detailed evidence precisely when and where it is needed. This dynamic, iterative evidence-gathering process avoids the critical information loss inherent in static methods and raises the upper bound on reasoning performance. Figure 1 (Right) demonstrates the practical benefit of this design on LSDBench (Qu et al., 2025), a benchmark specifically designed to test a model’s ability to find short, critical events in long videos. Our method achieves a better performance-efficiency trade-off, achieving superior accuracy compared to open source baselines while operating on a flexible and smaller frame budget.

Notably, training such an agent faces several challenges, a naive reinforcement learning approach would suffer from an inefficiently large action space and exhibit limited reasoning patterns. To address this, we introduce a two-stage training strategy. First, a cold-start Supervised Fine-Tuning (SFT) phase teaches the model the basics of tool usage. Using a tailored dataset of exemplar trajectories, we train the model to understand the task format, master the syntax of tool calls, and develop a baseline reasoning capability. Crucially, to prevent the model from merely imitating a single, monotonous reasoning pattern, we enrich this dataset with reflection data, which exposes our model to more diverse and sophisticated problem-solving strategies. Second, with these foundational skills established, a Reinforcement Learning (RL) phase optimizes the model’s tool interaction policy and reasoning capability, transforming it from a simple imitator into an adaptive agent that can generalize its strategy to unseen videos and questions.

We summarize our contributions as follows:

- We propose VideoZoomer, a novel framework that reframes long video understanding as a sequential tool interaction task, enabling an MLLM to dynamically control its visual focus via multi-turn tool interaction.
- We introduce a robust, two-stage training strategy: a cold-start phase using a tailored dataset of exemplar and reflection trajectories, followed by a reinforcement learning phase to optimize an efficient and effective agentic policy.
- We demonstrate through extensive experiments that our model significantly outperforms existing open-source models on a wide range of long video understanding and reasoning benchmarks, in some cases even surpassing leading proprietary models with greater efficiency.

108

2 RELATED WORKS

110 **Multimodal Reasoning Models.** The remarkable success in LLMs (Guo et al., 2025; Team et al.,
 111 2025; Tan et al., 2025; Jaech et al., 2024; Yang et al., 2025) has demonstrated that reinforcement
 112 learning (RL) is a powerful paradigm for enhancing the complex reasoning capabilities. Many works
 113 since then have tried to transfer this into multimodal domain. Methods such as MM-Eureka (Meng
 114 et al., 2025) and VL-Rethinker (Wang et al., 2025) have successfully adapted RL techniques to
 115 improve the vision-language reasoning abilities of MLLMs. More recently, Video-R1 (Feng et al.,
 116 2025) further validated the efficacy of this approach specifically within the video domain. Recently
 117 some works have tried further extend MLLMs with external tools like image cropping (Zheng et al.,
 118 2025; Su et al., 2025), web search (Wu et al., 2025), segmentation (Liu et al., 2025b). However,
 119 most of these methods focus on image tasks and only interact with the environment for single turn,
 120 combining RL-driven reasoning and multi-turn tool use strategy for long video understanding is still
 121 underexplored.

122 **Long Video Comprehension.** Many works have tried to extend the ability of MLLMs in long
 123 video comprehension. A stream of research aims to reduce the number of visual tokens that need to
 124 be fed into the MLLM (Liu et al., 2025a; Yan et al., 2025) through compression or selection mod-
 125 ules. A second, related approach focuses on selecting a sparse subset of the most salient frames from
 126 the entire video. Unlike uniform sampling, these methods aim to identify moments of high impor-
 127 tance (Tang et al., 2025; Hu et al., 2025a; Wang et al., 2024b). While effective, the primary limitation
 128 of these methods is that the frame selection process is decoupled with its reasoning process, hinder-
 129 ing it from learning more complex reasoning patterns. Methods like LongVILA-R1 (Chen et al.,
 130 2025) focus on direct context extension by continuing training on long video datasets to handle
 131 longer video sequences. Recently, a promising direction has emerged that leverages the powerful
 132 zero-shot capabilities of large proprietary models to act as agents. Frameworks like VideoDeepRe-
 133 search (Yuan et al., 2025) and Deep Video Discovery (Zhang et al., 2025) use prompting techniques
 134 to guide a strong LLM like Deepseek-R1 (Guo et al., 2025) or GPT 4.1 (OpenAI, 2024) to iter-
 135 atively explore a video with external tools. These training-free methods demonstrate the potential
 136 of agentic approach but rely on resource-intensive, closed-source models, making them difficult to
 137 optimize, reproduce, or deploy. In contrast, our work focuses on explicitly training a relatively small
 138 7B open-source model to learn an efficient, agentic policy for long video comprehension.

139

3 METHOD

140

3.1 OVERVIEW

141 To address the challenge of efficient long video understanding with a constrained frame budget, we
 142 propose a novel framework, VideoZoomer, which empowers a large multimodal model to actively
 143 seek high-temporal-resolution information by invoking an external tool. Rather than relying on fixed
 144 or uniform sampling strategies, our model learns to dynamically and adaptively allocate its frame
 145 budget during its reasoning process. The core idea is to train an agent that learns an optimal policy
 146 for when and where to request high-frame-rate video clips, a process we call “temporal zoom-in”,
 147 to gather sufficient evidence for answering a given question.

148 As illustrated in Figure 2, the **strategy** is summarized as “first glance, then zoom”: initially the
 149 model only has access to the query prompt Q and a relatively low frame rate version of the video
 150 V_{low} , uniformly sampled as a default frame rate f_{low} , which provides a coarse, computationally
 151 inexpensive overview of the entire video. To answer the question accurately, especially when it
 152 pertains to fine-grained temporal events or rapid motions, the model may require more detailed
 153 visual information. We introduce a `<video_zoom>` tool, which allows the model to request a
 154 specific time segment $[t_{start}, t_{end}]$ from the original video at a higher frame rate, f_{high} . Upon
 155 invoking this tool, the environment returns a high-resolution clip $V_{clip} = T(V, t_{start}, t_{end}, f_{high})$.
 156 The agent’s objective is to interact with the environment by iteratively calling the tool to gather
 157 visual evidence, this process continues until the agent determines it has sufficient information to
 158 produce a final answer. The agentic approach enables the model to develop diverse and complex
 159 reasoning strategies, as demonstrated in Figure 3. Each tool calling is constrained by a frame budget
 160 B (i.e. $f_{high} \times (t_{end} - t_{start}) \leq B$), thus the total number of frames that can be requested from the

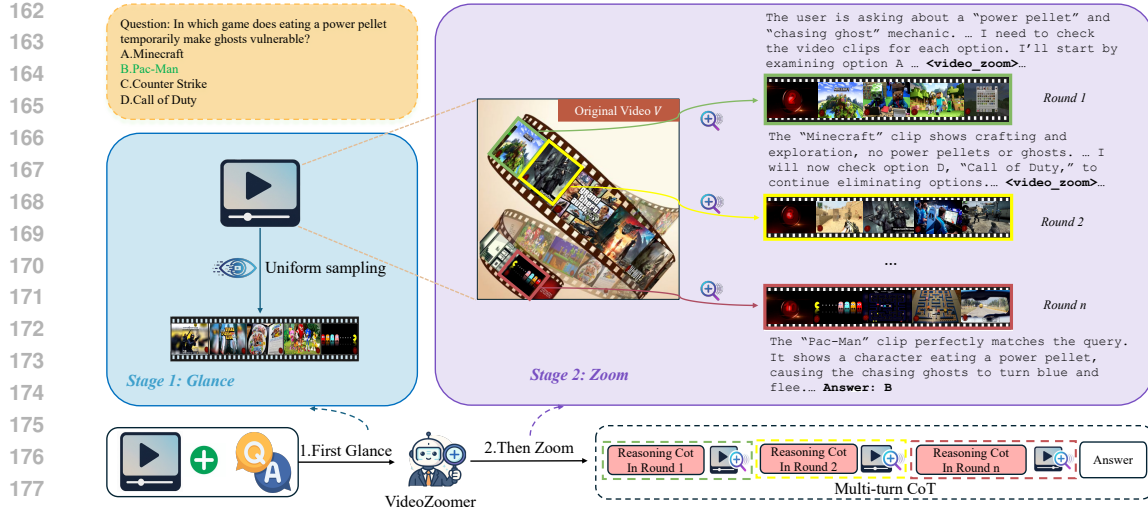


Figure 2: **VideoZoomer framework for long video reasoning.** The process begins with a “Glance” where the model obtains a coarse overview of the video. It then enters an iterative “Zoom” phase, where it can invoke a `<video_zoom>` tool to request high-fps clips and perform multi-turn reasoning. This process continues until the model produces a final answer or reaches max turn limit.

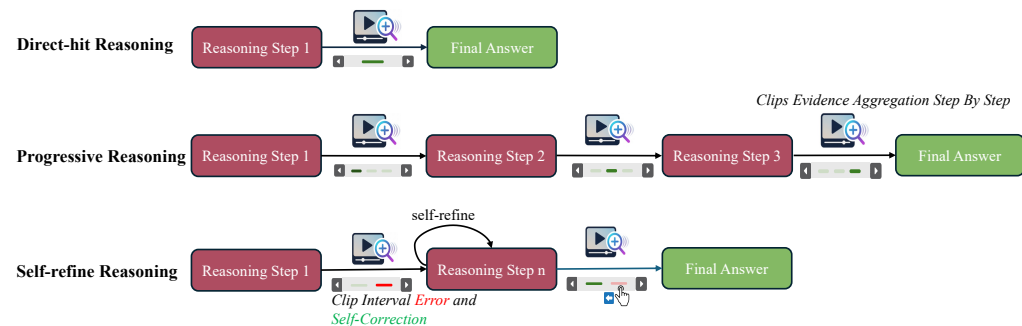


Figure 3: **Diverse reasoning patterns demonstrated by our model.** (a) Direct-hit Reasoning, (b) Progressive Reasoning, and (c) Self-refine Reasoning.

high-resolution clips is limited by $B \times N$, where N is the maximum number of interaction rounds. The environment returns an error message if the model makes an illegal request or exceeds the frame budget. The goal is to learn a policy π that maximizes the quality of the final answer while adhering to the frame budget and tool call number constraints.

3.2 COLD-START INITIALIZATION

Reinforcement learning from scratch on a complex, high-dimensional action space, such as generating structured tool calls, is notoriously sample-inefficient and prone to instability. To mitigate these challenges, we precede the RL phase with a supervised fine-tuning (SFT) stage designed to “cold-start” our agent. The primary objective of this stage is twofold: first, to equip a base multimodal model with the fundamental capability of understanding and invoking the `<video_zoom>` tool in the correct format; and second, to expose it to a diverse range of reasoning patterns, which is crucial for effective exploration during subsequent RL training. To achieve this, we construct a specialized SFT dataset by curating high-quality, multi-turn interaction trajectories as illustrated in Figure 4.

Distillation of Exemplar Trajectories. The initial step is to generate a set of “golden” tool-use trajectories. We leverage state-of-the-art proprietary models, such as GPT-4o (OpenAI, 2024) and Gemini-2.5-pro (Comanici et al., 2025), as expert demonstrators. For each video-question pair in our training set, we prompt the expert model with the same system prompt and initial low-frame-

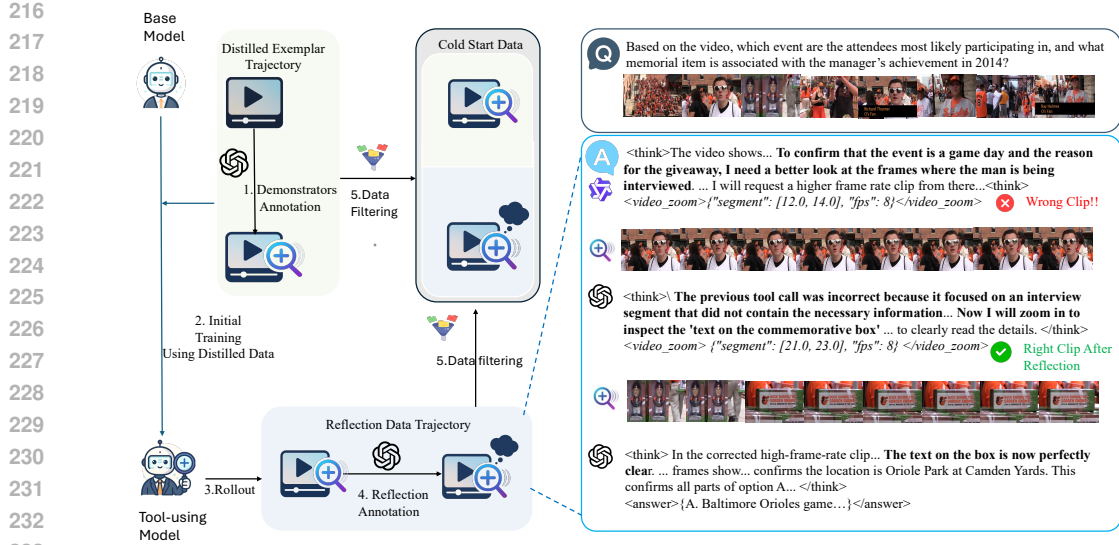


Figure 4: **The pipeline for curating our cold-start dataset.** We first distill exemplar trajectories, then generate reflection data by having an expert model correct the failures of an initial agent. The final dataset combines both verified exemplar and reflection trajectories.

rate video provided to our agent. The model then engages in a multi-turn interaction, iteratively calling the `<video_zoom>` tool until it gathers sufficient information to answer the question. This process yields a collection of complete trajectories, each containing the initial prompt, a sequence of tool calls, the corresponding high-frame-rate clip observations, and the final answer. These expert-generated trajectories serve as ideal examples of effective tool invocation and reasoning.

Augmentation with Reflection Data. While SFT on only exemplar trajectories effectively teaches the model the format of tool use, we observed a significant limitation: the resulting model tends to overfit the expert model’s dominant reasoning patterns. This often leads to a “shallow” policy, where the model learns to call the tool at most once and then immediately outputs an answer, regardless of whether the retrieved clip was actually helpful or contained errors. This lack of perseverance and adaptability would severely hinder its ability to solve more complex problems requiring deeper, iterative reasoning.

To address this and introduce more diverse and complex reasoning patterns, we generate reflection data. As shown in Figure 4. The process begins by using our initial model trained only on exemplar data, to produce its own rollouts. We then identify trajectories where the model failed to answer correctly. These incorrect rollouts are subsequently fed back to the expert model, which is prompted to reflect on the flawed reasoning. The model then identifies the mistake and generates a corrected, more robust reasoning path. This corrected path might involve additional tool calls or a different line of reasoning. This reflection process creates valuable training instances that explicitly teach the model how to recover from errors, critically evaluate the information returned by a tool, and when to persist with further investigation. Furthermore, this on-policy-like data generation strategy ensures that the new trajectories are challenging yet achievable, mitigating distribution shift and stabilizing the transition from SFT to RL.

The final cold-start dataset is a carefully curated combination of the distilled exemplar trajectories and reflection trajectories. Before inclusion, all candidate trajectories are passed through verifiers to ensure quality. This resulted composite dataset, approximately 11,000 trajectories in total, provides a rich and balanced foundation for our base model.

3.3 MULTI-TURN TOOL-INTEGRATED REINFORCEMENT LEARNING

We employ GRPO (Shao et al., 2024) for RL training due to its demonstrated efficacy in enhancing multimodal reasoning capabilities. We extend its original formula to multi-turn tool calling contexts

270 and adapt a token-level loss mask on tool call trajectory, ignoring text and image tokens that are not
 271 generated by the model.
 272

273 **Reward Design.** The design of the reward function is essential to guide the agent toward the
 274 desired behavior. Our reward is assigned at the end of each trajectory and is composed of three
 275 distinct components designed to promote accuracy, valid format, and exploration:
 276

$$R(x, y) = R_{acc}(x, y) + R_{format}(y) + R_{tool}(y) \quad (1)$$

277 The accuracy reward R_{acc} is the primary task-oriented reward, it provides a strong positive signal
 278 if the agent’s final answer is correct. The format reward R_{format} validates the structure of the
 279 agent’s response at each turn. This reward is set to a positive value if the model’s output strictly
 280 adheres to the predefined format, and zero otherwise. Specifically, the agent receives a positive
 281 reward if every intermediate step correctly wraps its reasoning in `<think></think>` tags and
 282 be followed by either a valid `<video_zoom></video_zoom>` or a final answer enclosed in
 283 `<answer></answer>` tags. A key challenge during early training is that a model unfamiliar
 284 with the `<video_zoom>` tool may be hesitant to use it, often preferring to guess an answer di-
 285 rectly. To solve this and encourage exploration, we introduce a bonus R_{tool} for using the tool. To
 286 prevent the agent from learning to make redundant or unhelpful tool calls, this bonus is conditional:
 287 it is only awarded if the final answer is correct.
 288

290 4 EXPERIMENT

291 4.1 EXPERIMENTAL SETUP

293 **Implementation Details.** We initialize our model from Qwen-2.5-VL-7B-Instruct (Bai et al.,
 294 2025) for its strong foundational capabilities and amenability to reinforcement learning. For cold-
 295 start initialization, we adapt the LLaMA-Factory (Zheng et al., 2024) framework. Our RL training
 296 and evaluation framework is based on verl (Sheng et al., 2024), which we extended to support multi-
 297 turn tool-calling tasks and optimized for efficiency in long video training scenario.
 298

299 For training data, we use LongVideoReason (Chen et al., 2025), a long video QA dataset comprised
 300 of 52K high-quality question-reasoning-answer pairs. In cold start stage, we trained our base model
 301 with a learning rate of 5×10^{-6} for 1 epoch on dataset we construct as described in Section 3.2.
 302 During RL stage, we use a learning rate of 1×10^{-6} , rollout number of 16 and batchsize of 128.
 303 The model is initialized with 64 uniformly sampled frames. It can then perform up to 4 subsequent
 304 tool calls, each retrieving up to 16 frames of high-resolution clip from a segment of interest, before
 305 providing a final answer. To improve training effectiveness and stability of RL training process,
 306 we also adapt clip-higher and dynamic sampling from DAPO (Yu et al., 2025). Further details are
 307 provided in the appendix.
 308

308 **Benchmarks.** To comprehensively evaluate the capabilities of our model, we conducted tests
 309 on two distinct categories of benchmarks: long video understanding and long video reason-
 310 ing. For long video understanding, we utilized four benchmarks: MLVU (Zhou et al., 2024),
 311 LongVideoBench (Wu et al., 2024), VideoMME (Fu et al., 2024), and LVBench (Wang et al., 2024a).
 312 These benchmarks encompass a variety of tasks designed to assess the model’s general video com-
 313 prehension abilities. For long video reasoning, we employed three benchmarks that require more
 314 than superficial visual analysis: VideoMMLU (Song et al., 2025), VideoMMU (Hu et al., 2025b),
 315 and LongVideoReason-eval (Chen et al., 2025). These chanllenging benchmarks are specifically
 316 designed to evaluate the model’s integrated perception and reasoning capabilities.
 317

318 4.2 MAIN RESULT

319 **Baselines.** We compare VideoZoomer against a wide range of video understanding models, in-
 320 cluding (1) Proprietary models: GPT-4o (OpenAI, 2024) and Gemini-1.5-Pro (Reid et al., 2024);
 321 (2) Open-source VLMs: Video-LLaVA (Lin et al., 2023), LLaVA-NeXT-Video (Zhang et al.,
 322 2024b), Video-XL (Shu et al., 2024), VILA-1.5 (Lin et al., 2024), Kangaroo (Liu et al., 2024a),
 323 LongVU (Shen et al., 2024), LongVA (Zhang et al., 2024a), LongVILA (Xue et al., 2024),
 324 LongVILA-R1 (Chen et al., 2025), Video-R1 (Feng et al., 2025) and Qwen2.5-VL (Bai et al., 2025).
 325

324 **Table 1: Results on long video benchmarks.**[†] denotes evaluation results using our own evaluation
 325 protocol under max frames of 128. For a fair comparison, our model is evaluated with a maximum
 326 of 64 frames in the first round, followed by up to 4 turns requesting a maximum of 16 frames per
 327 turn, yielding a total of max 128 frames.

Model	Size	Long Video Understanding						Long Video Reasoning		
		MLVU		LongVideoBench		VideoMME	LVBench	VideoMMLU	VideoMMU	LongVideoReason
		dev	test	val	overall	long	quiz	eval		
<i>Proprietary Models</i>										
GPT-4o	-	64.6	54.9	66.7	71.9	65.3	48.9	44.9	61.2	60.7
Gemini-1.5-Pro	-	-	-	64.0	75.0	67.4	33.1	-	53.9	67.3
<i>Open-Source VLMs</i>										
Video-LLaVA	7B	36.2	30.7	37.6	39.9	-	-	-	-	-
LLaVA-OneVision	7B	64.7	47.2	56.4	58.3	46.7	-	33.4	33.9	-
LLaVA-NeXT-Video	7B	-	-	49.1	-	-	-	27.6	-	-
Video-XL	7B	64.9	45.5	50.7	55.5	-	-	-	-	-
VILA-1.5	7B	56.7	-	-	-	-	-	20.5	20.9	-
Kangaroo	8B	61.0	-	54.8	56.0	-	<u>39.4</u>	-	-	-
LongVU	7B	<u>65.4</u>	-	-	60.6	-	-	-	-	-
LongVA	7B	56.3	41.1	-	52.6	-	-	-	24.0	-
LongVILA	7B	-	-	57.1	60.1	-	-	-	-	-
LongVILA-R1	7B	-	-	<u>57.6</u>	62.4	53.3	-	-	-	67.9
Video-R1 [†]	7B	65.0	<u>49.2</u>	52.0	61.1	51.4	38.7	<u>61.3</u>	<u>49.8</u>	<u>72.8</u>
Qwen2.5-VL [†]	7B	58.3	45.5	51.0	<u>63.5</u>	<u>53.9</u>	36.9	61.0	48.1	70.8
VideoZoomer [†]	7B	68.8	55.8	57.7	65.2	55.8	41.5	67.9	52.2	80.3
Δ over base model		+10.5	+10.3	+6.7	+1.7	+1.9	+4.6	+6.9	+4.1	+9.5

349 **Table 2: Detailed result on MLVU.** ER: Ego Reasoning. NQA: Needle QA, PQA: Plot QA, SQA:
 350 Sport QA, AO: Action Order, AC: Action Count, TQA: Tutorial QA, AR: Anomaly Recognition,
 351 TR: Topic Reasoning.

Split	Model	Single Detail				Multi-detail			Holistic		Avg.
		ER	NQA	PQA	SQA	AO	AC	TQA	AR	TR	
Dev	Qwen2.5-VL	47.7	65.1	65.9	-	50.2	13.6	-	65.5	85.6	58.3
	VideoZoomer	66.8	80.3	72.9	-	59.8	50.5	-	52.5	83.3	68.8
Test	Qwen2.5-VL	32.1	53.3	54.0	44.4	32.9	15.0	37.2	38.5	80.2	45.5
	VideoZoomer	58.5	63.3	64.0	44.4	42.9	28.3	39.5	46.2	89.0	55.8

360 **Long Video Understanding.** Our model demonstrates marked improvements across a range of
 361 long video understanding benchmarks, as shown in Table 1. On MLVU, it achieves scores of 69.0
 362 (dev) and 56.0 (test), yielding substantial gains of +10.5 and +10.3 points over its base model,
 363 Qwen2.5-VL. This performance is further validated on LongVideoBench and LVBench, where our
 364 model scores 57.7 and 41.5, respectively, outperforming all listed open-source baselines. These
 365 results collectively underscore the effectiveness of our adaptive temporal zoom mechanism. Not-
 366 ably, even on benchmarks not exclusively focused on extremely long durations like VideoMME, our
 367 method provides a clear performance boost (65.2 overall, 55.8 on long-set) over an already strong
 368 baseline. This demonstrates that the learned policy to dynamically “zoom” in relevant segments is
 369 beneficial across various video length.

370 We present a detailed analysis of our model’s performance on the MLVU benchmark in Table 2.
 371 The results clearly show that our method’s improvements are most significant on tasks requiring
 372 detailed perception. For instance, in the “Single Detail” category of the dev set, our model shows
 373 massive gains in Ego Reasoning (ER, +19.1), Needle QA (NQA, +15.2), and Plot QA (PQA, +7.0).
 374 The most significant improvement is seen in the “Multi-detail” task of Action Count (AC), where
 375 our model’s score increases from 13.6 to 50.5. This task, which requires counting specific, often
 376 rapid actions, directly benefits from the ability to re-sample critical moments at a higher frame rate.
 377 Similar substantial gains are observed on the test set in ER (+26.4), NQA (+10.0), and AC (+13.3).

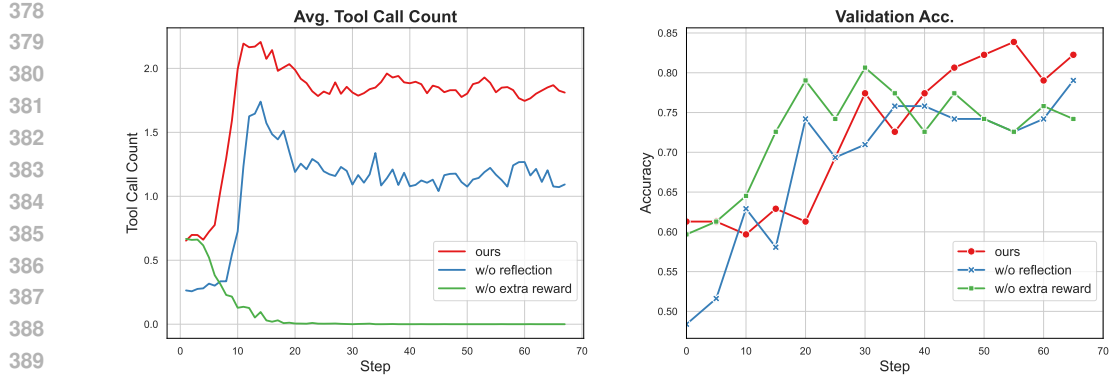


Figure 5: **Training dynamics of ablation baselines.** The left panel shows the average number of tool calls per sample during training. The right panel displays the model performance (e.g., accuracy) on the validation set over the course of training.

Table 3: **Evaluation of Ablation Baselines.**

Model	Long Video Understanding						Long Video Reasoning			
	MLVU		LongVideoBench		VideoMME		LVBench	VideoMMLU	VideoMMMU	LongVideoReason
	dev	test	val	overall	long		quiz		eval	
VideoZoomer	69.0	56.0	57.7	65.2	55.8	41.5	67.9	52.2	80.3	
w/o RL	56.4	45.6	42.0	54.4	44.2	26.0	63.5	46.6	63.3	
w/o R_{tool}	67.5	52.2	56.2	62.5	52.5	40.6	63.6	53.8	79.9	
w/o cold-start	57.0	42.8	43.5	53.5	46.6	35.5	63.9	43.6	59.6	
w/o reflection	67.0	53.2	54.8	58.7	47.4	40.9	70.1	52.2	75.1	

Long Video Reasoning. On VideoMMLU and VideoMMMU, our model scores 67.9 and 52.2 respectively, achieving the highest among all open-source models. On LongVideoReason-eval, our model achieves a highest score of 80.3, surpassing the performance of powerful proprietary models like GPT-4o (60.7) and Gemini-1.5-Pro (67.3). Notably, our model also outperforms LongVILA-R1, which is trained on the same dataset but with a larger frame budget, highlighting the superior efficiency of our agentic strategy. This indicates that the iterative, evidence-gathering process enabled by our agentic strategy allows the model to construct more robust and accurate reasoning chain, which is crucial for tackling complex, knowledge intensive video reasoning tasks.

4.3 ABLATION STUDY

Effectiveness of Key Components. To validate the contribution of each key component in our framework, we conduct a comprehensive ablation study, with results summarized in Table 3 and training dynamics shown in Figure 5. For a fair comparison, all ablated models except “w/o cold-start” were trained using the same amount of SFT data as our final model. The w/o RL model, trained only via supervised fine-tuning, suffers a catastrophic performance drop across all benchmarks (e.g., -17.0 on LongVideoReason), confirming that RL is essential for learning an effective tool-use policy. Similarly, the w/o cold-start model, which skips our curated SFT stage, fails to converge to a meaningful policy, highlighting the necessity of a strong initialization. Within the cold-start process, removing reflection data (w/o reflection) causes the model to adopt a shallow, simple strategy, where the average tool call count stabilizes at about 1.0, limiting its ability to tackle complex problems. In contrast, our full method learns to make nearly two calls on average, enabling deeper investigation and achieving higher accuracy in the validation set. Finally, removing the conditional tool-use bonus (w/o R_{tool}) leads to “policy collapse”, where the agent’s tool usage trends towards zero during training, as it fails to discover the tool’s utility without explicit encouragement.

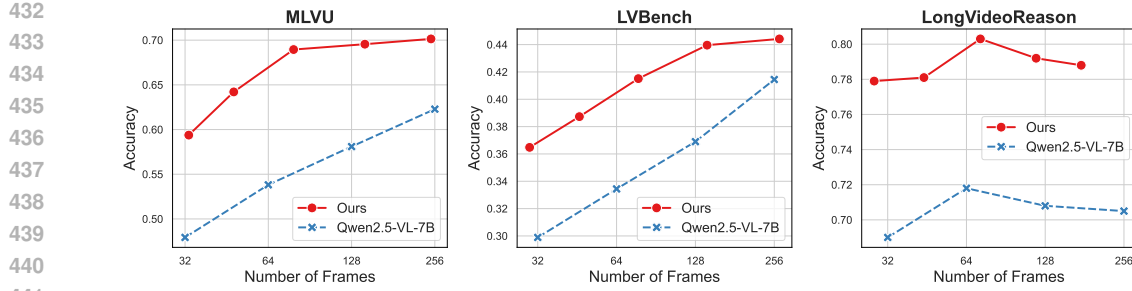


Figure 6: **Performance comparison with varying frame budgets.** We compare our model against the Qwen2.5-VL-7B baseline. The x-axis(log scale) represents the fixed frame budget for the baseline and the average number of frames actually used by VideoZoomer on each benchmark.

Each ablation results in significantly lower performance on various benchmarks, demonstrating that all components are necessary to achieve the final performance.

Performance Across Various Frame Budgets. To further investigate the efficiency of VideoZoomer, we analyze the performance of our model and the base model under various frame budgets. As illustrated in Figure 6, we plot the accuracy of the model against the number of frames processed. For the baseline model, this x-axis represents a fixed, uniformly sampled frame budget. For our model, it represents the actual average number of frames consumed per dataset, a result of its dynamic decision-making process. The results clearly demonstrate our model’s superior efficiency. On MLVU, our model achieves 0.64 accuracy using only 48 frames on average, surpassing the baseline’s 0.581 accuracy at a much larger 128 frame budget. This trend holds on LVBench, where our model using 77 frames outperforms the baseline using 256 frames. Furthermore, on the LongVideoReason benchmark, our model and the baseline model both peaks at around 64 frames, suggesting that complex reasoning tasks may not benefit from increasing visual information, which can introduce noise. However, within this optimal frame window, our model’s peak accuracy of 0.803 significantly surpasses the base model’s peak of 0.718. This performance gap underscores our model’s stronger reasoning capability enabled by its agentic policy.

Combining with a Frame Selector. Our primary method uses uniform sampling for the initial overview to ensure a global and unbiased starting point, we also investigate whether our agentic framework can be combined with more sophisticated frame selectors. To test this, we replace the initial uniformly sampled frames with the output of the output of TSPO-0.4B (Tang et al., 2025). The results presented in Table 4 shows that providing a more intelligently selected initial overview further boosts

our model’s performance by +1.8 on MLVU and +3.0 on LongVideoBench. This demonstrates the flexibility and transferability of our approach; the learned policy effectively leverages the improved starting point to conduct an even more efficient and accurate investigation of the video.

5 CONCLUSION

In this work, we propose VideoZoomer to address the critical challenge of long video understanding in MLLMs. We empower the MLLM to become an active agent capable of utilizing external tool to investigate long videos more effectively and efficiently through a carefully designed two-stage training process. Our experimental results robustly validated our approach. The ablation studies confirmed that each component—the cold-start initialization, the reflection data, the RL optimization, and the conditional reward bonus—was indispensable for achieving final performance. Our model not only achieves strong performance across numerous long video benchmarks, but also demonstrated superior frame efficiency, outperforming stronger baselines while using significantly fewer

486 frames. This demonstrates the effectiveness of our agentic strategy in enhancing the perception and
 487 reasoning capabilities of MLLMs for long videos.
 488

489 **ETHICS STATEMENT**
 490

491 Our research adheres to the ICLR Code of Ethics. This work aims to advance the efficiency of video
 492 understanding for positive applications, ensuring transparency, reproducibility, and fairness in all
 493 experiments. All datasets used are publicly available, and our use of proprietary models for data
 494 distillation complies with their terms of service. We acknowledge that our model, like other large
 495 language models, may inherit and reflect biases from its training data. While our method improves
 496 reasoning, it is not designed to mitigate social biases, and we advocate for responsible downstream
 497 use and further research into fairness. The intended application is for research purposes, and we do
 498 not foresee direct dual-use concerns from our proposed framework.
 499

500 **REPRODUCIBILITY STATEMENT**
 501

502 To ensure the reproducibility of our work, we provide a comprehensive overview of our methodol-
 503 ogy, implementation, and evaluation. Further implementation details, including training hyperpa-
 504 rameters and specific prompts used for training and data generation, are described in Appendix B.
 505 To facilitate direct replication and further research, we will release our codebase, datasets and model
 506 weight upon acceptance of this paper.
 507

508 **REFERENCES**
 509

510 Shuai Bai, Keqin Chen, Xuejing Liu, Jialin Wang, Wenbin Ge, Sibo Song, Kai Dang, Peng Wang,
 511 Shijie Wang, Jun Tang, et al. Qwen2. 5-vl technical report. *arXiv preprint arXiv:2502.13923*,
 512 2025.

514 Mu Cai, Reuben Tan, Jianrui Zhang, Bocheng Zou, Kai Zhang, Feng Yao, Fangrui Zhu, Jing Gu,
 515 Yiwu Zhong, Yuzhang Shang, et al. Temporalbench: Benchmarking fine-grained temporal under-
 516 standing for multimodal video models. *arXiv preprint arXiv:2410.10818*, 2024.

517 Wenhao Chai, Enxin Song, Yilun Du, Chenlin Meng, Vashisht Madhavan, Omer Bar-Tal, Jenq-
 518 Neng Hwang, Saining Xie, and Christopher D Manning. Auroracap: Efficient, performant video
 519 detailed captioning and a new benchmark. *arXiv preprint arXiv:2410.03051*, 2024.

521 Yukang Chen, Wei Huang, Baifeng Shi, Qinghao Hu, Hanrong Ye, Ligeng Zhu, Zhijian Liu,
 522 Pavlo Molchanov, Jan Kautz, Xiaojuan Qi, et al. Scaling rl to long videos. *arXiv preprint*
 523 *arXiv:2507.07966*, 2025.

525 Zhe Chen, Weiyun Wang, Yue Cao, Yangzhou Liu, Zhangwei Gao, Erfei Cui, Jinguo Zhu, Shen-
 526 glong Ye, Hao Tian, Zhaoyang Liu, Lixin Gu, Xuehui Wang, Qingyun Li, Yiming Ren, Zixuan
 527 Chen, Jiapeng Luo, Jiahao Wang, Tan Jiang, Bo Wang, Conghui He, Botian Shi, Xingcheng
 528 Zhang, Han Lv, Yi Wang, Wenqi Shao, Pei Chu, Zhongying Tu, Tong He, Zhiyong Wu, Hui
 529 Deng, Jiaye Ge, Kaiming Chen, Min Dou, Lewei Lu, Xizhou Zhu, Tong Lu, Dahu Lin, Yun-
 530 feng Qiao, Jifeng Dai, and Wenhui Wang. Expanding performance boundaries of open-source
 531 multimodal models with model, data, and test-time scaling. *ArXiv*, abs/2412.05271, 2024. URL
<https://api.semanticscholar.org/CorpusID:274581884>.

533 Gheorghe Comanici, Eric Bieber, Mike Schaeckermann, Ice Pasupat, Noveen Sachdeva, Inderjit
 534 Dhillon, Marcel Blstein, Ori Ram, Dan Zhang, Evan Rosen, et al. Gemini 2.5: Pushing the
 535 frontier with advanced reasoning, multimodality, long context, and next generation agentic capa-
 536 bilities. *arXiv preprint arXiv:2507.06261*, 2025.

538 Kaituo Feng, Kaixiong Gong, Bohao Li, Zonghao Guo, Yibing Wang, Tianshuo Peng, Junfei Wu,
 539 Xiaoying Zhang, Benyou Wang, and Xiangyu Yue. Video-r1: Reinforcing video reasoning in
 mllms. *arXiv preprint arXiv:2503.21776*, 2025.

540 Chaoyou Fu, Yuhan Dai, Yondong Luo, Lei Li, Shuhuai Ren, Renrui Zhang, Zihan Wang, Chenyu
 541 Zhou, Yunhang Shen, Mengdan Zhang, et al. Video-mme: The first-ever comprehensive evalua-
 542 tion benchmark of multi-modal llms in video analysis. *arXiv preprint arXiv:2405.21075*, 2024.
 543

544 Daya Guo, Dejian Yang, Haowei Zhang, Junxiao Song, Ruoyu Zhang, Runxin Xu, Qihao Zhu,
 545 Shirong Ma, Peiyi Wang, Xiao Bi, et al. Deepseek-r1: Incentivizing reasoning capability in llms
 546 via reinforcement learning. *arXiv preprint arXiv:2501.12948*, 2025.

547 Kai Hu, Feng Gao, Xiaohan Nie, Peng Zhou, Son Tran, Tal Neiman, Lingyun Wang, Mubarak
 548 Shah, Raffay Hamid, Bing Yin, et al. M-llm based video frame selection for efficient video
 549 understanding. In *Proceedings of the Computer Vision and Pattern Recognition Conference*, pp.
 550 13702–13712, 2025a.

551 Kairui Hu, Penghao Wu, Fanyi Pu, Wang Xiao, Yuanhan Zhang, Xiang Yue, Bo Li, and Ziwei
 552 Liu. Video-mmmu: Evaluating knowledge acquisition from multi-discipline professional videos.
 553 *arXiv preprint arXiv:2501.13826*, 2025b.

554

555 Aaron Jaech, Adam Kalai, Adam Lerer, Adam Richardson, Ahmed El-Kishky, Aiden Low, Alec
 556 Helyar, Aleksander Madry, Alex Beutel, Alex Carney, et al. Openai o1 system card. *arXiv
 557 preprint arXiv:2412.16720*, 2024.

558 Tim C Kietzmann, Patrick McClure, and Nikolaus Kriegeskorte. Deep neural networks in com-
 559 putational neuroscience. *bioRxiv*, 2018. URL <https://api.semanticscholar.org/CorpusID:195946461>.

560

561 Woosuk Kwon, Zhuohan Li, Siyuan Zhuang, Ying Sheng, Lianmin Zheng, Cody Hao Yu, Joseph E.
 562 Gonzalez, Hao Zhang, and Ion Stoica. Efficient memory management for large language model
 563 serving with pagedattention. In *Proceedings of the ACM SIGOPS 29th Symposium on Operating
 564 Systems Principles*, 2023.

565

566 Bin Lin, Yang Ye, Bin Zhu, Jiaxi Cui, Munan Ning, Peng Jin, and Li Yuan. Video-llava: Learning
 567 united visual representation by alignment before projection. *arXiv preprint arXiv:2311.10122*,
 568 2023.

569

570 Ji Lin, Hongxu Yin, Wei Ping, Pavlo Molchanov, Mohammad Shoeybi, and Song Han. Vila: On
 571 pre-training for visual language models. In *Proceedings of the IEEE/CVF conference on computer
 572 vision and pattern recognition*, pp. 26689–26699, 2024.

573

574 Jiajun Liu, Yibing Wang, Hanghang Ma, Xiaoping Wu, Xiaoqi Ma, Xiaoming Wei, Jianbin Jiao,
 575 Enhua Wu, and Jie Hu. Kangaroo: A powerful video-language model supporting long-context
 576 video input. *arXiv preprint arXiv:2408.15542*, 2024a.

577

578 Xiangrui Liu, Yan Shu, Zheng Liu, Ao Li, Yang Tian, and Bo Zhao. Video-xl-pro: Reconstructive
 579 token compression for extremely long video understanding. *arXiv preprint arXiv:2503.18478*,
 2025a.

580

581 Yuanxin Liu, Shicheng Li, Yi Liu, Yuxiang Wang, Shuhuai Ren, Lei Li, Sishuo Chen, Xu Sun,
 582 and Lu Hou. Tempcompass: Do video llms really understand videos? *arXiv preprint
 583 arXiv:2403.00476*, 2024b.

584

585 Yuqi Liu, Bohao Peng, Zhisheng Zhong, Zihao Yue, Fanbin Lu, Bei Yu, and Jiaya Jia. Seg-
 586 zero: Reasoning-chain guided segmentation via cognitive reinforcement. *arXiv preprint
 587 arXiv:2503.06520*, 2025b.

588

589 Fanqing Meng, Lingxiao Du, Zongkai Liu, Zhixiang Zhou, Quanfeng Lu, Daocheng Fu, Tiancheng
 590 Han, Botian Shi, Wenhai Wang, Junjun He, et al. Mm-eureka: Exploring the frontiers of multi-
 591 modal reasoning with rule-based reinforcement learning. *arXiv preprint arXiv:2503.07365*, 2025.

592

593 OpenAI. Gpt-4o. <https://openai.com/index/hello-gpt-4o/>, May 2024.

Tianyuan Qu, Longxiang Tang, Bohao Peng, Senqiao Yang, Bei Yu, and Jiaya Jia. Does your vision-
 language model get lost in the long video sampling dilemma? *arXiv preprint arXiv:2503.12496*,
 2025.

594 Machel Reid, Nikolay Savinov, Denis Teplyashin, Dmitry Lepikhin, Timothy P. Lillicrap, Jean-
 595 Baptiste Alayrac, Radu Soricut, Angeliki Lazaridou, Orhan Firat, Julian Schrittweiser, Ioannis
 596 Antonoglou, Rohan Anil, Sebastian Borgeaud, Andrew M. Dai, Katie Millican, Ethan Dyer, Mia
 597 Glaese, Thibault Sottiaux, Benjamin Lee, Fabio Viola, Malcolm Reynolds, Yuanzhong Xu, James
 598 Molloy, Jilin Chen, Michael Isard, Paul Barham, Tom Hennigan, Ross McIlroy, Melvin Johnson,
 599 Johan Schalkwyk, Eli Collins, Eliza Rutherford, Erica Moreira, Kareem Ayoub, Megha Goel,
 600 Clemens Meyer, Gregory Thornton, Zhen Yang, Henryk Michalewski, Zaheer Abbas, Nathan
 601 Schucher, Ankesh Anand, Richard Ives, James Keeling, Karel Lenc, Salem Haykal, Siamak
 602 Shakeri, Pranav Shyam, Aakanksha Chowdhery, Roman Ring, Stephen Spencer, Eren Sezener,
 603 and et al. Gemini 1.5: Unlocking multimodal understanding across millions of tokens of context.
 604 *CoRR*, abs/2403.05530, 2024.

605 Zhihong Shao, Peiyi Wang, Qihao Zhu, Runxin Xu, Junxiao Song, Xiao Bi, Haowei Zhang,
 606 Mingchuan Zhang, YK Li, Yang Wu, et al. Deepseekmath: Pushing the limits of mathemati-
 607 cal reasoning in open language models. *arXiv preprint arXiv:2402.03300*, 2024.

608 Xiaoqian Shen, Yunyang Xiong, Changsheng Zhao, Lemeng Wu, Jun Chen, Chenchen Zhu, Zechun
 609 Liu, Fanyi Xiao, Balakrishnan Varadarajan, Florian Bordes, et al. Longvu: Spatiotemporal adap-
 610 tive compression for long video-language understanding. *arXiv preprint arXiv:2410.17434*, 2024.

611 Guangming Sheng, Chi Zhang, Zilingfeng Ye, Xibin Wu, Wang Zhang, Ru Zhang, Yanghua Peng,
 612 Haibin Lin, and Chuan Wu. Hybridflow: A flexible and efficient rlhf framework. *arXiv preprint*
 613 *arXiv: 2409.19256*, 2024.

614 Yan Shu, Peitian Zhang, Zheng Liu, Minghao Qin, Junjie Zhou, Tiejun Huang, and Bo Zhao.
 615 Video-xl: Extra-long vision language model for hour-scale video understanding. *arXiv preprint*
 616 *arXiv:2409.14485*, 2024.

617 Enxin Song, Wenhao Chai, Weili Xu, Jianwen Xie, Yuxuan Liu, and Gaoang Wang. Video-mmlu:
 618 A massive multi-discipline lecture understanding benchmark. *arXiv preprint arXiv:2504.14693*,
 619 2025.

620 Alex Su, Haozhe Wang, Weiming Ren, Fangzhen Lin, and Wenhui Chen. Pixel reasoner: In-
 621 centivizing pixel-space reasoning with curiosity-driven reinforcement learning. *arXiv preprint*
 622 *arXiv:2505.15966*, 2025.

623 Huajie Tan, Yuheng Ji, Xiaoshuai Hao, Minglan Lin, Pengwei Wang, Zhongyuan Wang, and
 624 Shanghang Zhang. Reason-rft: Reinforcement fine-tuning for visual reasoning. *arXiv preprint*
 625 *arXiv:2503.20752*, 2025.

626 Canhui Tang, Zifan Han, Hongbo Sun, Sanping Zhou, Xuchong Zhang, Xin Wei, Ye Yuan, Jinglin
 627 Xu, and Hao Sun. Tspo: Temporal sampling policy optimization for long-form video language
 628 understanding. *arXiv preprint arXiv:2508.04369*, 2025.

629 Kimi Team, Angang Du, Bofei Gao, Bowei Xing, Changjiu Jiang, Cheng Chen, Cheng Li, Chenjun
 630 Xiao, Chenzhuang Du, Chonghua Liao, et al. Kimi k1. 5: Scaling reinforcement learning with
 631 llms. *arXiv preprint arXiv:2501.12599*, 2025.

632 Haozhe Wang, Chao Qu, Zuming Huang, Wei Chu, Fangzhen Lin, and Wenhui Chen. Vi-
 633 rethinker: Incentivizing self-reflection of vision-language models with reinforcement learning.
 634 *arXiv preprint arXiv:2504.08837*, 2025.

635 Weihuan Wang, Zehai He, Wenyi Hong, Yean Cheng, Xiaohan Zhang, Ji Qi, Xiaotao Gu, Shiyu
 636 Huang, Bin Xu, Yuxiao Dong, et al. Lvbench: An extreme long video understanding benchmark.
 637 *arXiv preprint arXiv:2406.08035*, 2024a.

638 Xijun Wang, Junbang Liang, Chun-Kai Wang, Kenan Deng, Yu Lou, Ming C Lin, and Shan Yang.
 639 Vila: Efficient video-language alignment for video question answering. In *European Conference*
 640 *on Computer Vision*, pp. 186–204. Springer, 2024b.

641 Haoning Wu, Dongxu Li, Bei Chen, and Junnan Li. Longvideobench: A benchmark for long-context
 642 interleaved video-language understanding. *arXiv preprint arXiv:2407.15754*, 2024.

648 Jinming Wu, Zihao Deng, Wei Li, Yiding Liu, Bo You, Bo Li, Zejun Ma, and Ziwei Liu. Mmsearch-
 649 r1: Incentivizing lmms to search. *arXiv preprint arXiv:2506.20670*, 2025.

650 Fuzhao Xue, Yukang Chen, Dacheng Li, Qinghao Hu, Ligeng Zhu, Xiuyu Li, Yunhao Fang, Haotian
 651 Tang, Shang Yang, Zhijian Liu, et al. Longvila: Scaling long-context visual language models for
 652 long videos. *arXiv preprint arXiv:2408.10188*, 2024.

653 Shilin Yan, Jiaming Han, Joey Tsai, Hongwei Xue, Rongyao Fang, Lingyi Hong, Ziyu Guo, and
 654 Ray Zhang. Crosslmm: Decoupling long video sequences from lmms via dual cross-attention
 655 mechanisms. *arXiv preprint arXiv:2505.17020*, 2025.

656 An Yang, Anfeng Li, Baosong Yang, Beichen Zhang, Binyuan Hui, Bo Zheng, Bowen Yu,
 657 Chang Gao, Chengan Huang, Chenxu Lv, et al. Qwen3 technical report. *arXiv preprint*
 658 *arXiv:2505.09388*, 2025.

659 Yixin Ye, Zhen Huang, Yang Xiao, Ethan Chern, Shijie Xia, and Pengfei Liu. Limo: Less is more
 660 for reasoning. *arXiv preprint arXiv:2502.03387*, 2025.

661 Kexin Yi, Chuang Gan, Yunzhu Li, Pushmeet Kohli, Jiajun Wu, Antonio Torralba, and Joshua B
 662 Tenenbaum. Clevrer: Collision events for video representation and reasoning. *arXiv preprint*
 663 *arXiv:1910.01442*, 2019.

664 Qiying Yu, Zheng Zhang, Ruofei Zhu, Yufeng Yuan, Xiaochen Zuo, Yu Yue, Weinan Dai, Tiantian
 665 Fan, Gaohong Liu, Lingjun Liu, et al. Dapo: An open-source llm reinforcement learning system
 666 at scale. *arXiv preprint arXiv:2503.14476*, 2025.

667 Sicheng Yu, Chengkai Jin, Huanyu Wang, Zhenghao Chen, Sheng Jin, Zhongrong Zuo, Xiaolei Xu,
 668 Zhenbang Sun, Bingni Zhang, Jiawei Wu, et al. Frame-voyager: Learning to query frames for
 669 video large language models. *arXiv preprint arXiv:2410.03226*, 2024.

670 Huaying Yuan, Zheng Liu, Junjie Zhou, Hongjin Qian, Ji-Rong Wen, and Zhicheng Dou.
 671 Videodeepresearch: Long video understanding with agentic tool using. *arXiv preprint*
 672 *arXiv:2506.10821*, 2025.

673 Hang Zhang, Xin Li, and Lidong Bing. Video-llama: An instruction-tuned audio-visual language
 674 model for video understanding. In *Conference on Empirical Methods in Natural Language Pro-*
 675 *cessing*, 2023. URL <https://api.semanticscholar.org/CorpusID:259075356>.

676 Peiyuan Zhang, Kaichen Zhang, Bo Li, Guangtao Zeng, Jingkang Yang, Yuanhan Zhang, Ziyue
 677 Wang, Haoran Tan, Chunyuan Li, and Ziwei Liu. Long context transfer from language to vision.
 678 *CoRR*, abs/2406.16852, 2024a.

679 Xiaoyi Zhang, Zhaoyang Jia, Zongyu Guo, Jiahao Li, Bin Li, Houqiang Li, and Yan Lu. Deep
 680 video discovery: Agentic search with tool use for long-form video understanding. *arXiv preprint*
 681 *arXiv:2505.18079*, 2025.

682 Yuanhan Zhang, Bo Li, haotian Liu, Yong jae Lee, Liangke Gui, Di Fu, Jiashi Feng, Ziwei Liu, and
 683 Chunyuan Li. Llava-next: A strong zero-shot video understanding model, April 2024b. URL
 684 <https://llava-vl.github.io/blog/2024-04-30-llava-next-video/>.

685 Yuanhan Zhang, Jinming Wu, Wei Li, Bo Li, Zejun Ma, Ziwei Liu, and Chunyuan Li. Video
 686 instruction tuning with synthetic data. *arXiv preprint arXiv:2410.02713*, 2024c.

687 Yaowei Zheng, Richong Zhang, Junhao Zhang, Yanhan Ye, Zheyuan Luo, Zhangchi Feng, and
 688 Yongqiang Ma. Llamafactory: Unified efficient fine-tuning of 100+ language models. In *Pro-*
 689 *ceedings of the 62nd Annual Meeting of the Association for Computational Linguistics (Volume*
 690 *3: System Demonstrations)*, Bangkok, Thailand, 2024. Association for Computational Linguis-
 691 *tics*. URL <http://arxiv.org/abs/2403.13372>.

692 Ziwei Zheng, Michael Yang, Jack Hong, Chenxiao Zhao, Guohai Xu, Le Yang, Chao Shen, and
 693 Xing Yu. Deepeyes: Incentivizing” thinking with images” via reinforcement learning. *arXiv*
 694 *preprint arXiv:2505.14362*, 2025.

695 Junjie Zhou, Yan Shu, Bo Zhao, Boya Wu, Shitao Xiao, Xi Yang, Yongping Xiong, Bo Zhang,
 696 Tiejun Huang, and Zheng Liu. Mlvu: A comprehensive benchmark for multi-task long video
 697 understanding. *arXiv preprint arXiv:2406.04264*, 2024.

702
703
704
705
A LLM USAGE
706
707
708
709
710
711
712

706 During the preparation of this paper, we utilized LLM to assist with grammar correction and lan-
707 guage refinement. In accordance with ICLR 2026 policy, we have carefully reviewed and edited all
708 model-generated text to ensure its accuracy and originality. The authors take full responsibility for
709 the final content of this paper.
710
711

712
713 B MORE IMPLEMENT DETAILS
714
715

716 **Evaluation Details.** We evaluate our model and baselines under a consistent setting with a maxi-
717 mum of 128 frames and a resolution corresponding to 100,352 pixels per frame. For inference, we
718 employed the vLLM framework (Kwon et al., 2023) with the temperature parameter set to 0 to en-
719 sure deterministic outputs. For the VideoMMLU benchmark, answers are scored by GPT-4o using
720 the official prompt and the final score is computed as the average score of three disciplines.
721
722

723 **Training Details.** We show the key training hyperparameters in Table 5.
724
725
726
727
728

Table 5: Key Hyperparameters

(a) SFT stage

729 730 731 732 733 734 735 736 737 Hyperparameter	730 731 732 733 734 735 736 737 Value
Train epochs	1
Train batch size	64
Learning rate	5e-5
Learning rate scheluder	cosine
Warmup ratio	0.1
Freeze vision encoder	true

(b) RL stage

729 730 731 732 733 734 735 736 737 Hyperparameter	730 731 732 733 734 735 736 737 Value
Max total response length	32768
Rollout temperature	1.0
Max interaction turns	5
Train batch size	128
PPO mini batch size	32
Rollouts per prompt (n)	16
Clip ratio (low / high)	0.2 / 0.27
Entropy coefficient	0.001
KL coefficient (β)	0.001
Learning rate	1e-6
Reward weight (acc/format/tool)	0.9/0.1/0.5

745 The SFT training is conducted on $8 \times$ H100 GPUs for ~ 6 h, RL training is conducted on $16 \times$ H100
746 GPUs for ~ 45 h.
747

748 Figure 7 shows key statistics of our cold-start dataset. The left panel shows the distribution of total
749 token lengths per trajectory, indicating a wide variety of response lengths that cover both simple and
750 complex reasoning chains. The right panel illustrates the distribution of interaction rounds (i.e., the
751 number of tool calls), showing that the dataset contains a significant number of multi-step examples.
752
753

754 **Prompt Template.** We provide the detailed prompt used for training and cold-start data synthe-
755 sization as follows:

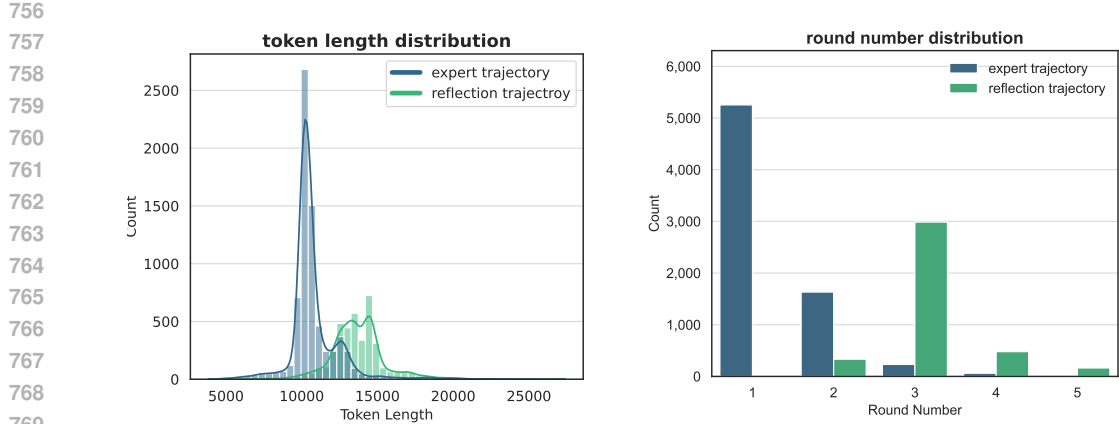


Figure 7: Statistics of the cold start dataset.

Reasoning Prompt

System Prompt: You are a helpful assistant. You will receive a low-frame-rate video and related questions. You can analyze the video content to answer the question and trigger high-frame-rate inspections when finer temporal resolution is needed. When you detect ambiguous motion/objects that require closer inspection, wrap your request in `<video_zoom></video_zoom>` tags and provide the exact time segment and target frame rate in JSON format: `<video_zoom>{"segment": [start_sec, end_sec], "fps": n}</video_zoom>`, it will return the video clip at the target fps to help you better answer the question. Note that the total frames num of the request clip cannot exceed 16 (e.g. $(end_sec - start_sec) * \text{fps} \leq 16$) and DO NOT include `<answer>` tags in this round. Example usage: `<video_zoom> {"segment": [4.0, 6.0], "fps": 2}</video_zoom>`. If the initial tool response does not provide sufficient information to answer the question, you may continue to request additional video zoom inspections as needed, until you either (1) gather enough information to form a complete answer, or (2) are explicitly instructed to stop using the tool. Output the thinking process within `<think> </think>` tags, once you confirm your final answer place the final answer inside `<answer>` and `</answer>`.

User: ...<framei_timet><image>...Question

Prompt for Constructing Reflection Trajectory

You are an expert video understanding model with access to a video zoom tool that allows you to request high-frame-rate clips for temporal inspection. Your task is to correct a flawed analysis of a low-frame-rate video by using a `video_zoom` tool. Your workflow is a multi-turn process:

Turn 1: Reflection and Tool Call

- Analyze the Error:** You will be given a question, choices, and a previous, incorrect attempt. First, you must reflect on *why* the previous `video_zoom` tool call was flawed. Was the time segment wrong? Was the frames-per-second (fps) too low? Was the focus of the analysis misaligned with the question?
- Formulate a Correction:** Based on your analysis, decide on a new, corrected `video_zoom` request. This request should target the precise moment of interest and use an appropriate fps to capture the fine-grained detail.
- Output the Tool Call:** Generate your reflection and the new tool call in the specified format. **Your output for this turn MUST end immediately after the `</video_zoom>` tag.** Do not generate anything further. The system will then execute this call and provide you with the result.

Constraint for the tool call: The total number of frames requested must not exceed 16. That is: $(end_sec - start_sec) * \text{fps} \leq 16$.

Turn 2: Analysis and Final Answer

- Receive Tool Response:** The system will provide the high-frame-rate video clip from your corrected tool call.

810
 811 2. **Analyze the New Clip:** Carefully examine the new clip. Describe what you can now clearly
 812 see that resolves the question.
 813 3. **Provide the Final Answer:** Based on your new observation, state the correct answer from the
 814 choices, enclosed in `\boxed{}`.
 815 **Output Format Structure:**
 816 **[FIRST TURN OUTPUT]**
 817 `<think>`
 818 The previous tool call was incorrect because [explain the flaw in the tool use, e.g., wrong segment,
 819 wrong fps, or misaligned focus].
 820 Now I will zoom in to inspect the motion of '{target object/action}' between {start_sec}s and
 821 {end_sec}s with higher temporal resolution.
 822 `</think><video_zoom> {"segment": [start_sec, end_sec], "fps": n}`
 823 **[YOUR TURN 1 OUTPUT STOPS HERE]**
 824 **[SECOND TURN OUTPUT] (after you receive the tool response)**
 825 `<think>` In the corrected high-frame-rate clip, [describe what is clearly observed now]. `</think>`
 826 **Example to follow:**
 827 **Question:** Which hand did the woman use to pick up the cup?
 828 **Choices:** A: Left hand B: Right hand C: Both hands D: Neither
 829 **Previous Trajectory (Wrong):** Tool call: `<video_zoom> {"segment": [0.0, 2.0],`
 830 `"fps": 2}</video_zoom>`
 831 **(Your First Turn Output Should Look Like This):**
 832 `<think>` The previous tool call was incorrect because it focused on the wrong time segment. The
 833 woman only reaches for the cup between 3.0s and 5.0s. Additionally, the low fps of 2 might not be
 834 sufficient to clearly distinguish the hand's motion.
 835 Now I will zoom in to inspect the motion of 'the woman's hand reaching for the cup' between 3.0s
 836 and 5.0s with a higher temporal resolution. `</think><video_zoom> {"segment": [3.0,`
 837 `10.0], "fps": 1}</video_zoom>`
 838 **(System provides tool response, then you start your Second Turn) (Your Second Turn Output**
 839 **Should Look Like This):**
 840 `<think>`In the corrected high-frame-rate clip, the woman's right hand is clearly seen moving towards
 841 and gripping the cup handle between 4.1s and 4.8s, while her left hand remains on her lap. The motion
 842 is now unambiguous. `</think> <answer> B. </answer>`

842 C MORE EXPERIMENT RESULTS

844 C.1 DIFFERENT EXPERT MODEL FOR COLD-START DATA CONSTRUCTION.

846 In our main experiments, we utilized data distilled from Gemini 2.5 Pro to generate the cold-start
 847 SFT dataset. To justify this choice, we conduct a comparative analysis of data distilled from Gemini
 848 2.5 pro versus data from GPT-4o. We conducted two identical training runs of our model. The only
 849 difference was the source of the cold start dataset used in the SFT stage: one model was trained on
 850 data distilled from GPT-4o, and the other on data from Gemini 2.5 Pro. Both models then underwent
 851 the same reinforcement learning phase. We evaluated the final performance of both models on our
 852 key benchmarks. The results of this comparison are presented in Table 6. As the result shows, the
 853 model trained using data from Gemini 2.5 pro achieved slightly better results on most benchmarks.
 854 Through qualitative analysis of the generated data, we observed that the trajectories from Gemini
 855 exhibited greater diversity in their reasoning patterns and tool-use strategies.

856 Table 6: Performance comparison using different expert models for cold-start data construction.

858 Model	859 Size	860 MLVU		861 LongVideoBench		862 VideoMME		863 LVBench		864 VideoMMLU		865 VideoMMMU		866 LongVideoReason	
		867 dev	868 test	869 val	870 overall	871 long	872 quiz	873 eval	874 eval	875 eval	876 eval	877 eval	878 eval		
879 Qwen2.5-VL	880 7B	881 58.1	882 45.4	883 51.0	884 63.5	885 53.9	886 36.9	887 61.0	888 48.1	889 70.8	890	891	892	893	
894 VideoZoomer _{gemini}	895 7B	896 68.8	897 55.8	898 57.7	899 65.2	900 55.8	901 41.5	902 67.9	903 52.2	904 80.3	905	906	907	908	
909 VideoZoomer _{gpt-4o}	910 7B	911 69.5	912 54.6	913 55.5	914 61.6	915 51.0	916 41.2	917 64.1	918 51.2	919 78.4	920	921	922	923	

864 C.2 RESULTS ON OOD TASKS
865866 To assess the generalizability and robustness of VideoZoomer, we evaluated its performance on two
867 distinct out-of-distribution (OOD) task categories: short video captioning and logical reasoning on
868 synthetic data. These experiments were designed to verify that our training process enhances long-
869 video capabilities without degrading the model’s foundational abilities.870 While our primary focus is on long videos, we tested VideoZoomer on several short video captioning
871 benchmarks TemporalBench(Cai et al., 2024),TempCompass(Liu et al., 2024b) and VDC(Chai et al.,
872 2024) to ensure its core descriptive capabilities were maintained. The results, summarized in Table 7,
873 show that our model not only preserves but significantly improves upon the baseline’s performance
874 across all tested benchmarks.875 Table 7: Short Video Captioning Benchmark Results
876877

878 Model	879 TemporalBench (Short Caption Score)	880 TempCompass (Captioning Acc)	881 VDC (Short Acc / Score)
880 QwenVL-2.5-7B	881 40.9	882 52.1	37.8 / 1.98
882 VideoZoomer	56.4	65.3	49.2 / 2.51

883 We further tested the model’s robustness on a subset of the CLEVRER dataset(Yi et al., 2019), which
884 evaluates causal and logical reasoning on synthetic videos. This domain is significantly different
885 from the real-world, long-form videos used in our training.886 As shown in Table 8, the comparable performance to the baseline model demonstrates that our two-
887 stage training process does not degrade the model’s foundational reasoning abilities. The minimal
888 gain is expected, as the glance-and-zoom mechanism is not designed for the abstract, logical puzzles
889 presented by CLEVRER. This result confirms that our method successfully retains the model’s core
890 competencies on tasks that do not require our agentic framework.893 Table 8: Performance on CLEVRER
894895

896 Model	897 CLEVRER Accuracy
897 QwenVL-2.5-7B	67.3
898 VideoZoomer	68.0

901 C.3 IMPACT OF SFT DATA QUANTITY
902903 We investigated whether the effectiveness of our Supervised Fine-Tuning (SFT) phase stems from
904 the quantity of data. We compared our model, trained on our curated 11k trajectory dataset, against
905 a model trained on a dataset of the same composition but with double the quantity (~20k samples).907 Table 9: Impact of SFT Data Quantity
908909

910 Training Dataset	911 MLVU (dev)	912 MLVU (test)	913 LVBench	914 LongVideoBench	915 LongVideoReason-eval
Ours (~11k)	68.8	55.8	41.5	57.7	80.3
Scaled Dataset (~20k)	69.5	54.6	41.2	55.5	78.4

916 As shown in Table 9, simply doubling the data quantity did not lead to better overall performance.
917 While there was a marginal improvement on MLVU (dev), the model trained on the larger dataset
918 performed worse on all other benchmarks. This result strongly suggests that the effectiveness of our
919 dataset comes from the high-quality, diverse reasoning patterns it contains, rather than its sheer size.
920 This “less is more” philosophy aligns with recent findings from works like DeepSeek-R1(Guo et al.,

918 2025) and LIMO(Ye et al., 2025), which demonstrate that a few thousand high-quality, reasoning-
 919 focused samples can be sufficient to unlock powerful capabilities in large models. Our methodology
 920 prioritizes a rich collection of reasoning pathways over a large volume of repetitive examples.
 921

922 C.4 ANALYSIS OF CHOSEN FPS

923
 924 A key feature of our <video_zoom> tool is that the frames-per-second (fps) for a “zoom-in” clip
 925 is dynamically generated by the model itself, allowing it to decide not only where to look but also
 926 how closely to look. To understand the model’s learned behavior, we analyzed the distribution of
 927 fps values it chose across thousands of tool calls on our validation set.

928 The results in Table 10 reveal that the model does not default to the highest possible fps. Instead,
 929 its most frequent choice is a moderate fps in the (1, 2] range, which it selects in 66.2% of cases.
 930 This demonstrates that the model learns an efficient policy, requesting just enough temporal detail to
 931 solve the task without unnecessarily expending its frame budget. While a high fps like 8 might seem
 932 excessive for a full video, it is a reasonable and effective choice for examining a critical few-second
 933 clip, and the model learns to use it sparingly.

934
 935 Table 10: Distribution of fps Values Chosen by the Model
 936

937 fps Range	938 (0, 1]	939 (1, 2]	940 (2, 4]	941 (4, 8]	942 (8, ∞)
943 Percentage	944 24.9%	945 66.2%	946 8.2%	947 0.6%	948 $\leq 0.1\%$

949 C.5 PERFORMANCE BY MAXIMUM ALLOWED TOOL CALLS

950 To understand the impact of multi-step reasoning, we evaluated how model accuracy changes with
 951 the maximum number of allowed tool calls. We varied the limit from 0 (no tool use) to 4 and
 952 measured performance across several benchmarks.

953
 954 Table 11: Performance by Maximum Allowed Tool Calls
 955

956 Max Tool Calls	957 MLVU (dev)	958 MLVU (test)	959 LongVideoBench	960 LVBenchmark	961 LongVideoReason-eval
962 0 (No Tool Use)	963 65.0	964 52.6	965 52.7	966 38.7	967 64.8
968 1	969 66.7	970 53.4	971 55.3	972 39.6	973 79.9
974 2	975 67.8	976 56.6	977 57.0	978 41.4	979 80.2
980 3	981 68.4	982 56.0	983 56.2	984 41.8	985 81.1
986 4	987 69.0	988 55.8	989 57.7	990 41.5	991 80.3

992 The results in Table 11 show a clear trend. The most significant performance jump occurs when al-
 993 lowing just one tool call, confirming the fundamental value of our agentic framework. For example,
 994 on LongVideoReason-eval, accuracy leaps from 64.8% to 79.9%. Increasing the limit from one to
 995 two calls provides another consistent and significant boost, highlighting the importance of multi-turn
 996 interaction for refining searches or gathering more evidence. After two calls, the benefits of increas-
 997 ing the limit further show diminishing returns. While there are minor gains, the improvements are
 998 smaller and less consistent. Our final model, with a limit of 4, uses this extra budget sparingly for
 999 the hard problems, but the core performance is achieved within the first two interactions.

999 D MORE CASES

972

973

974

975

Q:How many green mugs were on the fridge top after I first opened the fridge?A. 0 B. 2 C. 3 D. 1

976

977

978

979

980

981

<think>The user is asking about the number of green mugs on the fridge top after the first time the fridge is opened. The relevant frames are around **342.83s**. I need to see the motion of the person opening the fridge and what is inside. I will request a higher frame rate clip from 342.0s to 343.0s.</think>

<video_zoom>{"segment": [342.0, 343.0], "fps": 8}</video_zoom>

982

983

984

985

986

987

988

989

990

991

992

993

994

995

996

997

998

999

1000

Figure 8: Case Study: Single-Detail Reasoning.

Q:What does the man do before frying the food at the end of the video?

- A. Adjusts the kitchen timer
- B. Cuts some vegetables
- C. Cleans the frying pan
- D. Melts butter
- E. Sprinkles some pepper on the food
- F. Turns on the range hood

1001

1002

1003

1004

1005

1006

1007

1008

1009

1010

1011

1012

1013

1014

1015

1016

1017

1018

1019

1020

1021

1022

1023

1024

1025

<think>The question is about the man's actions before frying the food. The relevant part of the video is towards the end, around 1640s. I need to see the sequence of events leading up to the frying to determine what he does first. I will request a higher frame rate clip for the segment from 1630s to 1640s.</think><video_zoom>{"segment": [1630.0, 1640.0], "fps": 1}</video_zoom>

<think>In the high-frame-rate clip, I can see the sequence of events clearly.- From 1630s to 1634s, the man is using a whisk to stir something in a pot.- At 1635s, he stops stirring and walks to the stove.- At 1638s, he picks up a stick of butter from a wooden bowl. At 1640s, he is seen adding the butter to a pan on the stove. This confirms that before he fries the food, he melts butter in the pan. The other options are not shown in this specific sequence.</think><answer>D</answer>

Figure 9: Case Study: Single-Detail Reasoning.

1026
1027
1028
1029
1030
1031
1032
1033
1034
1035
1036
1037
1038
1039

1040
1041
1042
1043
1044
1045
1046
1047
1048
1049
1050

Q: In accordance with the video footage, who protects the mermaid?



<think>The user is asking about who protects the mermaid. The initial frames show the mermaid and a shark together, but I need to see the sequence of events to understand the interaction and who is protecting her. I'll request a clip from around 30 seconds to see what happens next.</think>

<video_zoom>{"segment": [30.0, 32.0], "fps": 4}</video_zoom>



<think>The zoomed clip confirms that the shark is holding a drawing of the mermaid and the dog, which suggests that the shark is planning something. However, the clip does not show the immediate interaction or the protection of the mermaid. I need to request a clip from around 32 seconds to see what happens next.</think>

<video_zoom> {"segment": [32.0, 34.0], "fps": 4} </video_zoom>



<think>The zoomed clip shows that the shark is now standing next to the mermaid, and the dog is in the background. This confirms that the shark is actively protecting the mermaid, as the dog is not visible in the immediate vicinity. The interaction between the shark and the mermaid is clear, and the shark is clearly the one providing protection.</think>

<answer>\boxed{A. The shark.}</answer>

Figure 10: Case Study: Self-Correction and Refined Reasoning.

1065
1066
1067
1068
1069
1070
1071
1072
1073
1074
1075
1076
1077
1078
1079

1080

1081

1082

1083

1084 Q: Which of the following options correctly matches the sequence of actions as they actually appear
 1085 in the video?

1086 A. making jewelry --> cleaning toilet --> paragliding --> carving pumpkin
 1087 B. paragliding --> making jewelry --> cleaning toilet --> carving pumpkin
 1088 C. carving pumpkin --> cleaning toilet --> making jewelry --> paragliding
 1089 D. paragliding --> cleaning toilet --> carving pumpkin --> making jewelry



1090

1091

1092

1093

1094 <think>The user wants me to match the sequence of events presented in different time clips provided
 1095 in the video frames. To accurately match the sequence, I need to clarify the order of specific moments
 1096 mentioned in the question. A higher frame rate inspection around the relevant timestamps is necessary
 1097 to get precise details. I'll start with the segment where a paraglider is visible.</think>

1098 <video_zoom>{"segment": [50.0, 52.0], "fps": 8}</video_zoom>



1099

1100

1101

1102 <think>The first clip confirmed that the sequence includes paragliding. Next, I need to confirm the
 1103 order of the other specified activities\u2014making jewelry, cleaning a toilet, and carving pumpkins.
 1104 I'll zoom into another section where jewelry-making and cleaning the toilet are visible for better
 1105 details and context. I'll focus on the relevant timestamps for these activities.\n</think>

1106 <video_zoom> {"segment": [90.0, 92.0], "fps": 4}</video_zoom>



1107

1108

1109

1110 <think>The second clip confirms that the activity of making jewelry occurs before cleaning the toilet.
 1111 Now, I will inspect the segment where cleaning a toilet is visible to better understand the sequence
 1112 of these events. The cleaning clips usually appear towards the later part of the sequence
 1113 I will request a clip from around 180.0s to 182.0s to see the transition from the previous scene to
 1114 the next.</think><video_zoom> {"segment": [180.0, 182.0], "fps": 8}</video_zoom>



1115

1116

1117

1118 <think>The third clip confirms that the cleaning of the toilet follows the \u201cmaking
 1119 jewelry\u201d activity. Finally, I need to confirm the last action, which is carving a pumpkin. The
 1120 pumpkin carving is at the initial stages in the video sequence. I will now request a sequence around
 1121 the moment this specific activity is visible in greater detail.<think><video_zoom> {"segment": [279.0,
 1122 281.0], "fps": 8}</video_zoom>



1123

1124

1125

1126 <think>The zoomed clip confirms that carving the pumpkin is shown between 279.0s and 281.0s.
 1127 This confirms that carving the pumpkin is the final event in the sequence. Combining all the
 1128 observations, the correct sequence of events is paragliding, making jewelry, cleaning the toilet, and
 1129 carving the pumpkin.</think>

1130 <answer>B. paragliding --> making jewelry --> cleaning toilet --> carving pumpkin</answer>

1131

1132

1133

Figure 11: Case Study: Multi-Detail Reasoning for Complex Queries.

1134

1135

1136

1137

1138

1139

1140

1141

1142

1143

1144

1145

Based on the video, which event are the attendees most likely participating in, and what commemorative item is associated with the manager's 2014 achievement?

- A. A Baltimore Orioles home game at Camden Yards, featuring a 2014 AL Manager of the Year garden gnome giveaway
- B. A Baltimore Ravens playoff game, distributing Super Bowl commemorative footballs
- C. A Baltimore Orioles fan convention, offering signed baseballs by 2014 MVP players
- D. A charity event at a local park, giving away team jerseys from the 2014 season



1151

1152

1153



<think>The video shows a crowd at what appears to be a baseball stadium ("Camden Yards" is visible), primarily wearing orange "Orioles" shirts. Several frames show people handing out and presenting commemorative boxes. In the background, we see "Buck Showalter" on products. **Frame 11 confirms a "Buck Showalter Garden Gnome 2014 AL Manager of the Year."** The event is clearly associated with the Baltimore Orioles. To confirm that the event is a game day and the distribution is specifically for the manager's 2014 achievement, I need a better look at the frames where the man is being interviewed. The frame at timestamp 12s seems most relevant. **I will request a higher frame rate clip from there** to see the specific moment when the product is presented and the reason for the giveaway is mentioned.</think>

<video_zoom>{"segment": [12.0, 14.0], "fps": 8}</video_zoom>

1160

1161

1162



<think>\n\nThe previous tool call was incorrect because it focused on an interview segment that did not contain the necessary information to answer the question. The question requires identifying both the event and the specific commemorative item. While the video generally shows an Orioles event, **the previous call from 12s-14s only shows a fan talking and provides no details about the item itself. The crucial information is presented on the boxes being given away.** Frame 11 at 22.02s and frame 12 at 24.02s clearly show the item's box.\n\nNow I will zoom in to inspect the 'text on the commemorative box' between 21.0s and 23.0s with a higher temporal resolution to clearly read the details.\n</think>

<video_zoom> {"segment": [21.0, 23.0], "fps": 8}</video_zoom>

1163

1164

1165

1166

1167

1168

1169

1170

1171

1172

1173

1174

1175

1176

1177

1178

1179

1180

1181

1182

1183

1184

1185

1186

1187

Figure 12: Demonstration of cold start data.

1188

1189

1190

1191

1192

1193

1194

1195 Based on the video's content, which activity shown in the scenes is **not** one of the restrictions Saudi
 1196 Arabian women face according to the '10 Things that Saudi Arabian Women Still Cannot Do'?

1197 A. Driving a car independently
 1198 B. Voting in elections
 1199 C. Competing freely in sports
 1200 D. Marrying without male guardian consent



1201

1202

1203



1204 <think>\n1. The video lists '10 Things That Saudi Arabian Women Still Cannot Do'.\n2. The user wants to identify the activity among
 1205 the given list that is not one of the restrictions.\n3. I need to confirm what the video explicitly states as a restriction.\n\nLet's examine
 1206 the provided frames to see which of these activities appear in the video as a restriction:\n- Frame at 7 seconds: Shows a woman
 1207 driving, which is labeled 'NO. 7'.\n- Frame at 115 seconds: Shows text 'VOTING'.\n- Frame at 144 seconds: Shows women at a
 1208 market, with text 'MAKE-UP' on the left.\n- Frame at 194 seconds: Shows women looking at an abaya, with text '3.
 1209 WOMEN'S LOYALY'.\n- Other frames like 150s, 205s, 286s, 317s, 356s, and 362s also introduce other restrictions. However, there is
 1210 no explicit mention of the specific activity of protected 'white men so they can rightfully protect them'.\n\nThe restriction about men
 1211 having to be present for certain of women's actions to be protected explicitly mentions men. **It's clear from the provided frames that**
 1212 **voting appears explicitly as a restriction ('VOTING' at 115s).** This directly answers the question as B. Voting in elections is explicitly
 1213 mentioned as a restriction, and other options are mentioned previously in the video. I can see the relevant point about voting and
 1214 confirm it by requesting a higher frame rate clip.\n\nLet's inspect the segment around 100 seconds where 'VOTING' is first
 1215 presented. A request for more detailed frames here is appropriate.\n</think>
<video_zoom>{"segment": [101.0, 103.0], "fps": 7}</video_zoom>



1216

1217

1218

1219

1220

1221

1222

1223

1224



1225 <think>\n1. The previous tool call was incorrect because it focused on a completely irrelevant time segment. The call zoomed into 101.0s to 103.0s, which shows a woman getting her makeup done. This segment has no connection to any of the activities listed in
 1226 the question (driving, voting, sports, marriage). The analysis was therefore based on a flawed premise and a misaligned tool call.\n\nTo
 1227 answer the question correctly, I must first understand that the video lists all four options (A, B, C, and D) as restrictions. The
 1228 question asks which one is *not* a restriction, implying that the video itself provides visual evidence to contradict one of its own
 1229 points.\n- **Driving (A)** is listed as a restriction, but the video shows a woman driving, smiling, and making a peace sign (Frame 9, 53.39s).\n- **Voting (B)** is listed as a restriction (Frame 53, 314.48s).\n- **Competing in sports (C)** is listed as a restriction, but the
 1230 video shows female athletes at the Olympics (Frame 36, 213.61s and Frame 40, 237.34s).\n- **Marrying without consent (D)** is listed
 1231 as a restriction (Frame 46, 272.94s).\n\nBoth driving and sports show visual contradictions. However, the scene of the woman driving
 1232 and giving a peace sign is a very direct and celebratory piece of footage that strongly suggests this 'restriction' is being overcome or is
 1233 no longer in place. **I will zoom in on this specific moment to confirm the celebratory nature of the action, which would explain why**
 1234 **it's the correct answer.** The previous analysis completely missed this.\n\nNow I will zoom in to inspect the motion of 'the woman
 1235 driving the car' between 52.0s and 54.0s with a higher temporal resolution.\n</think>
<video_zoom>{"segment": [52.0, 54.0], "fps": 8}</video_zoom>



1236

1237

1238

1239

1240

1241



1242 <think>\n1. In the corrected high-frame-rate clip, I can now clearly see the sequence of events between 52.0s and 54.0s. A woman
 1243 in a headscarf and sunglasses is sitting in the driver's seat of a car. She turns towards the camera, smiles confidently, and
 1244 then raises her hand to make a 'peace' or 'victory' sign. The action is deliberate and celebratory. The video presents this scene,
 1245 along with others of women driving, immediately after listing 'Driving a Car' as restriction number 7. This visual evidence of a woman
 1246 driving happily and triumphantly directly contradicts the video's claim that this is something they 'still cannot do.' While other
 1247 activities like 'competing in sports' are also shown, the footage of the woman driving with a peace sign is a more direct and personal
 1248 refutation of the restriction presented in the video. The other listed restrictions do not have such a clear, contradictory visual
 1249 representation.\n</think>

<answer>\boxed{A}</answer>

Figure 13: Example of cold start data.